New Structural Insights into the Iron-Molybdenum Cofactor from *Azotobacter vinelandii* Nitrogenase through Sulfur K and Molybdenum L X-ray Absorption Edge Studies

Britt Hedman,[†] Patrick Frank,[‡] Stephen F. Gheller,[§] A. Lawrence Roe,[‡] William E. Newton,[§] and Keith O. Hodgson*[,‡]

Contribution from the Stanford Synchrotron Radiation Laboratory, SLAC, Bin 69, P.O. Box 4349, Stanford, California 94305, Department of Chemistry, Stanford University, Stanford, California 94305, and Western Regional Research Center, USDA—ARS, Albany, California 94710, and Department of Biochemistry and Biophysics, University of California, Davis, California 95616. *Received July 13, 1987*

Abstract: The electronic and structural nature of sulfur and molybdenum in the FeMo cofactor (FeMo-co) isolated from *Azotobacter vinelandii* MoFe protein has been studied by X-ray absorption edge and near-edge spectroscopy (referred to herein collectively as XANES) at the sulfur K and molybdenum L_3 and L_2 absorption edges. In contrast to the relatively poor resolution found for X-ray absorption edges at higher energies (e.g., several electronvolts at the molybdenum K edge at 20 keV), resolution in the 2.5–3.0-keV region is significantly improved (e.g., 0.5 eV at the sulfur K edge at 2.47 keV), resulting in more edge structure with higher sensitivity to changes in electronic and structural environment. In order to record spectra from dilute samples at these low energies, an experimental method that takes advantage of the higher flux synchrotron radiation from an undulator magnet has been developed. XANES spectra have been recorded for FeMo-co in the oxidized (ox) and semireduced (s-r) forms and, for comparison, a number of inorganic complexes containing molybdenum and sulfur. To remove the interference of dithionite, its decomposition products, and other small, unbound molecules from the FeMo-co spectrum, an anaerobic column chromatographic method of purification has been developed. The spectrum of dithionite-free FeMo-co in the oxidized form could thus be recorded. The results show that, in addition to the bridging sulfides, an unprecedented, oxidized form of sulfur bound to FeMo-co is present. Analysis reveals that the species shows a close correspondence with bound thiosulfate. It is also shown that chloride plays no part in ligation of FeMo-co. Finally, by comparison of both the molybdenum L and sulfur K edges of the oxidized and semireduced FeMo-co states with several Mo-Fe-S clusters, it is found that the oxidation state of molybdenum is unchanged upon redox. The results reported herein demonstrate a new method for FeMo-co purification and raise some important questions about the role of dithionite and its decomposition products in both the mechanism of extraction and the properties of FeMo-co.

The iron–molybdenum cofactor (FeMo-co) from nitrogenase is the extruded, putative N_2-reducing site of nitrogenase, the typical bacterial nitrogen fixation apparatus. The MoFe protein component of the enzyme complex contains two such cofactors,[1,2] each of which contains one molybdenum atom, six to eight iron atoms, and eight to nine sulfur atoms arranged in a heterometallic cluster unique to this enzyme.[3-5] Since its first extrusion from the protein matrix, FeMo-co has attracted much interest both on its own and as a means to probe the Mo environment of the enzyme. It has been studied by a wide variety of physical and chemical methods probing, among other things, its composition,[5] reactivity, oxidation–reduction properties,[6] and structure.[7,8]

The most recent, significant information concerning FeMo-co has been derived from X-ray absorption spectroscopy (XAS) and electrochemical studies. Both EXAFS[7] (extended X-ray absorption fine structure) and XANES[8] (X-ray absorption near-edge structure) at the Mo K edge have been used to derive structural information on FeMo-co, both within and after extraction from its protein matrix. These studies have shown the molybdenum in FeMo-co in the presence of excess dithionite to be coordinated by three oxygen/nitrogen atoms and three sulfur/chlorine atoms at about 2.12 and 2.37 Å, respectively, with about three iron atom neighbors at an average distance of about 2.70 Å. Iron XAS provides a similar picture.[9] The detailed electrochemical investigations[6] have indicated that isolated FeMo-co, just as does its protein-bound form,[1,10] undergoes two redox processes, interrelating the semireduced (s-r) redox state produced in the presence of excess dithionite, FeMo-co(s-r), with both a more oxidized form, FeMo-co(ox), and a more reduced form, FeMo-co(red). The reduced state, corresponding to the substrate-reducing level,[6] has not yet been stabilized outside the catalytically competent enzyme system. The oxidized to semireduced change in isolated FeMo-co is a reversible, one-electron transfer, which correlates with the appearance and loss of the biologically unique $S = {}^3/_2$ EPR signal.[6]

Even with the compilation of much analytical, reactivity, and spectroscopic data, information concerning the three-dimensional arrangement of the composite atoms of FeMo-co is lacking, as is insight into the redox state of its individual atoms, particularly molybdenum, and the ligands surrounding the Mo–Fe–S core of this entity. A continuing major concern pertains to the purity of FeMo-co preparations, particularly with respect to the presence of either molybdenum- or iron-containing degradation products, protein-derived contaminants, and other small molecules, either introduced by the preparation protocol or produced from the consumption of dithionite used as a protectant against the continual

[†] Stanford Synchrotron Radiation Laboratory.
[‡] Stanford University.
[§] USDA—ARS and University of California, Davis.

(1) Münck, E.; Rhodes, H.; Orme-Johnson, W. H.; Davis, L. C.; Brill, W. J.; Shah, V. K. *Biochim. Biophys. Acta* **1975**, *400*, 32.
(2) Euler, W. B.; Martinsen, J.; McDonald, J. W.; Watt, G. D.; Wang, Z.-C. *Biochemistry* **1984**, *23*, 3021.
(3) Yang, S.-S.; Pan, W.-H.; Friesen, G. D.; Burgess, B. K.; Corbin, J. L.; Stiefel, E. I.; Newton, W. E. *J. Biol. Chem.* **1982**, *257*, 8042.
(4) Shah, V. K.; Brill, W. *J. Proc. Natl. Acad. Sci. U.S.A.* **1977**, *74*, 3249.
(5) Nelson, M. J.; Levy, M. A.; Orme-Johnson, W. H. *Proc. Natl. Acad. Sci. U.S.A.* **1983**, *80*, 147.
(6) Schultz, F. A.; Gheller, S. F.; Burgess, B. K.; Lough, S.; Newton, W. E. *J. Am. Chem. Soc.* **1985**, *107*, 5364.
(7) Conradson, S. D.; Burgess, B. K.; Newton, W. E.; Mortenson, L. E.; Hodgson, K. O. *J. Am. Chem. Soc.* **1987**, *109*, 7507. Cramer, S. P.; Gillum, W. O.; Hodgson, K. O.; Mortenson, L. E.; Stiefel, E. I.; Chisnell, J. R.; Brill, W. J.; Shah, V. K. *J. Am. Chem. Soc.* **1978**, *100*, 3814. Cramer, S. P.; Hodgson, K. O.; Gillum, W. O.; Mortenson, L. E. *J. Am. Chem. Soc.* **1978**, *100*, 3398.
(8) Conradson, S. D.; Burgess, B. K.; Newton, W. E.; Hodgson, K. O.; McDonald, J. W.; Rubinson, J. F.; Gheller, S. F.; Mortenson, L. E.; Adams, M. W. W.; Mascharak, P. K.; Armstrong, W. A.; Holm, R. H. *J. Am. Chem. Soc.* **1985**, *107*, 7935.
(9) Antonio, M. R.; Teo, B.-K.; Orme-Johnson, W. H.; Nelson, M. J.; Groh, S. E.; Lindahl, P. A.; Kauzlarich, S. M.; Averill, B. A. *J. Am. Chem. Soc.* **1982**, *104*, 4703. Arber, J. M.; Flood, A. C.; Garner, C. D.; Hasnain, S. S.; Smith, B. E. *J. Phys. (Les Ulis, Fr.)* **1986**, *47*, C8-1159.
(10) Watt, G. D.; Burns, A.; Tennent, D. L. *Biochemistry* **1980**, *19*, 4926.

0002-7863/88/1510-3798$01.50/0

threat of rapid destruction of FeMo-co by dioxygen.

Insight into many of these problems is potentially available through the application of XANES studies. This technique is sensitive to both the electronic structure and the geometric arrangement of ligands around an absorbing site. It has already proven useful in addressing structural questions in biological systems including myoglobin,[11] plastocyanin,[12] and nitrogenase.[8] However, energy resolution is degraded for edges at high photon energies due to the combination of poorer monochromator resolution and core-hole lifetime effects, which hinders detailed studies of the edge structure of many important metalloproteins. Techniques to overcome these problems are being developed through study of X-ray absorption edges at lower photon energies where these resolution-degrading effects are less severe. Thus, molybdenum edge structure in the FeMo-co, which is unresolvable at the molybdenum K edge (20 keV),[8] can be more completely resolved at the L edges (2.5–2.9 keV). In addition, L-edge spectroscopy permits the study of both s (L_1) and p (L_2 and L_3) symmetry initial states, thereby enhancing the electronic information obtained. There is however, the disadvantage that spectral assignments of XANES features are difficult for even moderately complex molecules, and pending further advances in the theoretical description of edge structure,[13] information comes primarily from empirical correlations and study of systematic trends. Even without specific assignments, this information is significant in describing electronic and structural features of molybdenum and sulfur sites as illustrated herein.

The sulfur K and molybdenum L absorption edges occur at energies (2.4–2.9 keV) not easily accessible at synchrotron UHV or hard X-ray beam lines. By using the 54-pole wiggler beam line VI-2 at the Stanford Synchrotron Radiation Laboratory (SSRL) in undulator mode, i.e., at reduced magnetic fields for the insertion device, we have developed an experimental method[14] that produces sufficient photon flux at these energies to measure dilute biological samples under nonvacuum conditions.

Using the 54-pole wiggler in undulator mode gives flux enhancement due to several effects. Because of the spectral change caused by the lower magnetic fields, the thermal load on beam-line optics is reduced to a level permitting the removal of all the heat-absorbing graphite filters. These filters attenuate the low-energy photon flux almost completely under wiggler conditions. In addition, the three beam-line Be windows can be reduced in thickness (in the present study by 25% to 250, 125, and 25 μm). When the magnetic field of the wiggler is decreased to reach undulator mode (the so-called deflection parameter K approaches a value close to 1),[15] the continuous synchrotron radiation spectrum is changed to contain quasi-monochromatic peaks.[14] These maxima represent a magnetic field-dependent fundamental with related harmonics.[15] It is thus possible to adjust the magnetic field of the undulator such that a suitable harmonic is located at the X-ray absorption edge under study, giving a maximum flux enhancement for the specific experiment. The total gain in flux thus obtained is about 1 order of magnitude over that from an 8-pole wiggler beam line at SSRL and is in the range of 10^9 photons/s.

We have used this experimental method to measure the sulfur K and molybdenum L_3 and L_2 edge XANES of FeMo-co from *Azotobacter vinelandii* nitrogenase, the results of which are described below. The samples include FeMo-co in both oxidized and semireduced states. We have also carried out a systematic XANES study of a large number of organic and inorganic sulfur-containing compounds at the sulfur K edge and for those containing molybdenum in various symmetries and coordinations at the molybdenum L edges as well. The detailed results of these experiments will be presented in a forthcoming paper.[16] We report here the sulfur K and molybdenum L_3 and L_2 edge XANES of selected compounds that are relevant to the interpretation of the XANES from the FeMo-co. Comparisons with these compounds provide new insight into both ligation and the oxidized to semireduced redox process of FeMo-co.

Experimental Section

Sample Preparation and Handling of FeMo-co. The nitrogenase MoFe protein of *A. vinelandii* was purified to homogeneity as described.[17] The specific activity of the protein was 1925 nmol of C_2H_2 reduced/min per mg of protein. FeMo-co was prepared from this protein by the large-scale HCl/NaOH modification[3] of the original isolation method.[4] *N*-Methylformamide (NMF) was purified by stirring over Na_2CO_3 for 16 h, followed by filtration and vacuum distillation. NMF extracts of FeMo-co were concentrated by vacuum distillation followed by centrifugation to separate solid material. The FeMo-co solution had [Mo] = 3.5 mM, Fe:Mo = 6.5:1, and activity in the reconstitution assay[18] of 128 nmol of C_2H_2 reduced/min per nmol of Mo. The FeMo-co solution was prepared initially in the presence of 1–2 mM $Na_2S_2O_4$ to ensure full protection against destruction by dioxygen. However, the solution was then stored anaerobically in serum vials at −80 °C to allow for "self-oxidation"[6] before transport to SSRL. Three FeMo-co samples, labeled herein A–C, were run as solutions in NMF during two different experimental sessions at SSRL.

At SSRL each sample was thawed in a Vacuum Atmospheres inert-atmosphere (N_2), dry glovebox and transferred by syringe into sealed XAS cryostat cells having only Pt-coated and polypropylene surfaces in contact with the FeMo-co solution. The sample cell was enclosed in a second sample compartment through which a constant flow of He was maintained during the measurements. The sample was kept at +4 °C during the data collection. Following the XAS experiment, the sample was unloaded in the same glovebox, and aliquots were transferred to a serum vial, which was stored frozen at −80 °C until assayed, and to an EPR tube, which was frozen in liquid nitrogen to prevent self-oxidation.

For sample A, which was shown by EPR spectroscopy to be in its oxidized (ox) form when loaded into the cell, the post-XAS EPR spectrum clearly showed that photoreduction had taken place during the measurements. The XANES measurements were therefore repeated in the next experimental session with a sample (B) to which fresh basic dithionite solution (prepared as below) was added to FeMo-co just before being loaded into the XAS cell. EPR examination showed this sample to be in the semireduced (s-r) form both before the XAS experiment and after the measurement.

The remainder of sample B was recombined with unirradiated FeMo-co and treated as follows to give sample C. Dithionite and all other low-MW solutes were removed from the NMF solution of the FeMo-co sample by filtration through a column of Sephadex G-25 (Pharmacia). This column was prepared by thoroughly degassing dry G-25 with gentle warming on a high-vacuum line. The gel was then swelled in the glovebox with purified NMF containing 2 mM $Na_2S_2O_4$, added as a freshly prepared 200 mM solution in 1 mM aqueous NaOH. The poured column was washed free of sodium dithionite with purified NMF (2–3 column volumes). A 300-μl aliquot of 3.5 mM FeMo-co(s-r) was passed through the 10-mL bed volume column. The FeMo-co eluted as a green band in ~2.9 mL. The eluant was concentrated to ~230 μL under high vacuum with stirring and gentle warming (≤35 °C). This procedure generated the oxidized form of FeMo-co, as verified by EPR. An aliquot was taken for activity assay, and the remainder of this di-

(11) Congiu-Castellano, A.; Bianconi, A.; Dell'Ariccia, M.; Giovanelli, A.; Burattini, E.; Durham, P. J. *Springer Proc. Phys.* **1984**, *2*, 164.

(12) Scott, R. A.; Hahn, J. E.; Doniach, S.; Freeman, H. C.; Hodgson, K. O. *J. Am. Chem. Soc.* **1982**, *104*, 5364.

(13) The X-ray absorption near-edge region, XANES, is dominated above threshold by multielectron and multiple scattering processes that make the application of simple molecular orbital concepts of restricted use. There are a number of approaches to quantitative interpretation of this region, among the more successful of which are extensions of the SCF–Xα formalism. We have recently extended such calculations to the interpretation of sulfur K edges for relatively simple inorganic compounds such as SO_4^{2-}, $S_2O_3^{2-}$, and $S_2O_6^{2-}$: Tyson, T. A.; Roe, A. L.; Frank, P.; Hodgson, K. O.; Hedman, B., submitted for publication in *Phys. Rev. B: Condens. Matter*. The calculations correlate well with experiment and show in the case of $S_2O_3^{2-}$ that the transitions at 2472 eV and around 2480 eV derive from the liganding and central sulfurs, respectively.

(14) Hedman, B.; Frank, P.; Penner-Hahn, J. E.; Roe, A. L.; Hodgson, K. O.; Carlson, R. M. K.; Brown, G.; Cerino, J.; Hettel, R.; Troxel, T.; Winick, H.; Yang, J. *Nucl. Instrum. Methods Phys. Res., Sect. A* **1986**, *246*, 797.

(15) Brown, K.; Halbach, K.; Harris, J.; Winick, H. *Nucl. Instrum. Methods Phys. Res.* **1983**, *208*, 65. Winick, H.; Boyce, R.; Brown, G.; Hower, N.; Hussain, Z.; Pate, T.; Umbach, E. *Nucl. Instrum. Methods Phys. Res.* **1983**, *208*, 127.

(16) Hedman, B.; Frank, P.; Gheller, S. F.; Roe, A. L.; Penner-Hahn, J. E.; Newton, W. E.; Hodgson, K. O., manuscript in preparation.

(17) Burgess, B. K.; Jacobs, D. B.; Stiefel, E. I. *Biochim. Biophys. Acta* **1980**, *614*, 196.

(18) Brigle, K. E.; Weiss, M. C.; Newton, W. E.; Dean, D. R. *J. Bacteriol.* **1987**, *169*, 1547.

thionite-free sample (C) was then loaded in the XAS cell and XANES measurements were performed. A spectrum after the XAS measurements was EPR-silent, showing no photoreduction.

The activity assay[18] showed no loss in catalytic activity for any of the samples (A–C) after the XANES runs, demonstrating no loss of integrity.

Sample Preparation of Solid Samples. Sulfur (sublimed powder, J. T. Baker), $Na_2S_2O_3 \cdot 5H_2O$ (J. T. Baker), $MoO_2(C_5H_7O_2)_2$ (Alfa Products), $Na_2S_2O_4$ (Alfa), $Na_2S_4O_6 \cdot 2H_2O$ (Aldrich), L-cysteic acid monohydrate (Aldrich), Na_2SO_3 (Mallinckrodt), and $K_2S_2O_5$ (Alfa) were used as purchased. The following compounds were prepared by literature methods: $Mo_2S_4(N,N\text{-}Et_2dtc)_2$,[19] $Mo_2O_2S_2(N,N\text{-}Et_2dtc)_2$,[19] $Mo_2O_4(N,N\text{-}Et_2dtc)_2$,[19] $(NH_4)_2MoS_4$,[20] $(Et_4N)_3[Mo_2Fe_6S_8(OCH_3)_3(SC_6H_5)_6]$,[21] $(n\text{-}Bu_4N)_3[Mo_2Fe_6S_8(SC_6H_5)_9]$,[21] $(n\text{-}Bu_4N)_5[Mo_2Fe_6S_8(SC_6H_5)_9]$,[21] $(Et_4N)_2[Fe_4S_4(SCH_2C_6H_5)_4]$,[22] $(Et_4N)_2[Fe(S_2\text{-}o\text{-}xyl)_2]$,[23] $(Et_4N)[Fe(S_2\text{-}o\text{-}xyl)_2]$[23]. $(Et_4N)_3[Fe(MoS_4)_2]$,[24] and $(NH_4)_2Se(S_2O_3)_2 \cdot 1.5H_2O$,[25] where $N,N\text{-}Et_2dtc$ is diethyldithiocarbamate, $S_2\text{-}o\text{-}xyl$ is $\alpha,\alpha'\text{-}o$-xylenedithiolate, Me_4N is tetramethylammonium, Et_4N is tetraethylammonium, and $n\text{-}Bu_4N$ is tetra-n-butylammonium. All solid samples were ground to an extremely fine powder, which was dispersed thinly on Mylar tape (containing an acrylic adhesive that was determined to be free of sulfur and molybdenum contaminants), and mounted across the window of an Al plate. For the air-sensitive compounds this preparation was performed in the inert-atmosphere glovebox, the front of the sample sealed behind thin polypropylene film and the sample holder exposed to air less than 20 s while being transferred from a sealed jar into the He atmosphere of the sample compartment at the beam line.

Data Aquisition and Analysis. The sulfur K and molybdenum L absorption edge XANES were measured by using the 54-pole wiggler beam line VI-2 at SSRL in undulator mode (magnetic fields of 1.4–1.5 kG). The data were collected under dedicated conditions (3 GeV, 30–75 mA) with a Pt-coated focusing mirror and a Si(111) double-crystal monochromator. The data for some of the solid model compounds were measured with similar experimental setups but under unfocused conditions on the 8-pole wiggler beam lines IV-2 and VII-3 at SSRL. The monochromator was detuned ~30% (undulator) and 70–80% (8-pole wiggler) to eliminate higher harmonic components in the X-ray beam.

The data were collected as fluorescence excitation spectra utilizing an ionization chamber as fluorescence detector.[26,27] The entire beam path from the beam pipe to the detector window, including the I_0 ionization chamber, was filled with He atmosphere, and a minimum number of 6.35-μm thickness polypropylene windows used. The energy was calibrated from XANES spectra of elemental sulfur and of $Na_2S_2O_3 \cdot 5H_2O$, run at intervals between the samples. The so-called "white-line" maximum of the sulfur spectrum and the maximum of the first edge feature in the $S_2O_3^{2-}$ spectrum were assigned to 2472.7 and 2472.0 eV, respectively, corresponding to an inflection point of 2471.3 eV for sulfur. The consistency of this energy calibration between different experimental sessions on different beam lines was checked internally as well as against recorded XANES spectra of molybdenum and copper foil. In the edge region, the step size was ≤0.15 eV and the spectrometer resolution was ~0.5 eV. A reproducibility in edge position determination of better than 0.2 eV was obtained by calculating and comparing first and second derivatives of the spectra for model compounds measured during different experimental sessions.

A smooth preedge background was removed from the spectra by fitting a polynomial to the preedge region and subtracting this polynomial from the entire spectrum. The molybdenum L_3 edge (at ~2523 eV) is only ~50 eV higher in energy than the sulfur K edge (at ~2472 eV). For compounds containing both sulfur and molybdenum, the sulfur K near-edge structure and EXAFS superimpose upon the edge structure of the molybdenum L_3 edge, making a proper preedge subtraction impossible. In these cases, lines were fitted to either the pre- or postedge regions and subtracted. Particularly for the dithionite-containing FeMo-co samples, the effects of the sulfur EXAFS on the backgrounds were quite pronounced, though there is no ambiguity introduced into the interpretation or conclusions presented below. The spectra presented represent the average of individual scans (2–3 for solid model compounds; for FeMo-co samples A/B/C; 7/5/11 scans at sulfur K, 14/19/15 scans at molybdenum L_3, and 18/25/15 scans at molybdenum L_2, respectively).

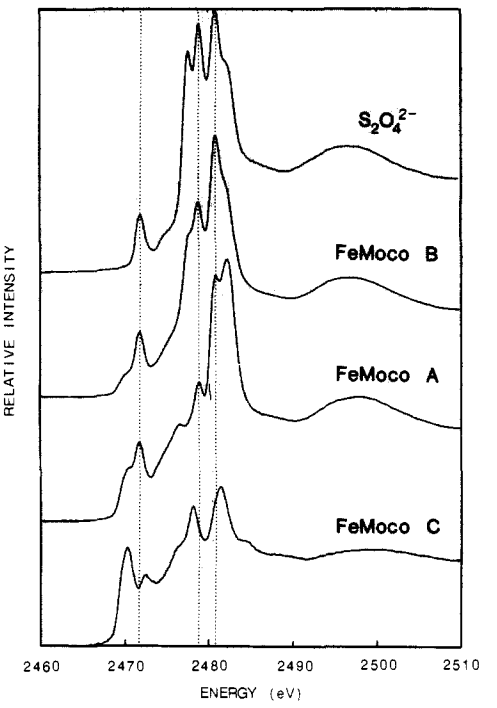

Figure 1. Sulfur K-edge XANES (top to bottom): the aged aerobic aqueous sodium dithionite solution of Figure 2, FeMo-co sample B, and FeMo-co sample A (each containing dithionite and/or its oxidation/decomposition products); FeMo-co sample C (dithionite-free). The striking resemblance between the two top spectra shows that the rapid production of thiosulfate in aqueous $S_2O_4^{2-}$ solutions has its parallel in NMF solutions such as that of the FeMo-co sample B. There is also a good correspondence for the peak positions of the first and third spectra. There is no overlap between dithionite-related transitions in the top spectrum and the transitions for sample C. The first transition in all FeMo-co spectra (at ~2470 eV) has no equivalent in the dithionite spectrum.

Results and Discussion

XANES studies were performed for three FeMo-co samples at both the sulfur K and molybdenum L_3 and L_2 edges. All these samples had been self-oxidized (in dry ice at −80 °C). Sample A, though in the oxidized state initially, was converted to the semireduced state by photoreduction in the beam. Sample B contained fresh basic dithionite and was in the semireduced state throughout the experiment. Sample C, which was purified free of dithionite, its oxidation/decomposition products, and other small unbound molecules and ions, was in the oxidized state throughout. For comparison with the FeMo-co spectra, XANES measurements were also performed for a wide variety of sulfur compounds, with sulfur in different oxidation states and coordination geometries and bound to oxygen, carbon, sulfur, selenium, or transition metals. XANES spectra of a large number of molybdenum compounds having oxygen, nitrogen, and/or sulfur ligation were also recorded, representing different coordination geometries and formal oxidation states, and included Fe–S and Mo–Fe–S cubane clusters.[21-23] A detailed description of the X-ray absorption spectroscopic results at the sulfur K, and molybdenum L_3, L_2, and L_1 absorption edges is presently in preparation.[16] We will summarize when appropriate the trends observed as a basis for the interpretation of the XANES of FeMo-co.

Sulfur K Edge. The sulfur K-edge XANES is characterized by white-line features, which derive primarily from 1s → 3p transitions.[13] Mixing with 3d states is also possible. The edge

(19) Schultz, F. A.; Ott, V. R.; Rolison, D. S.; Bravard, D. C.; McDonald, J. W.; Newton, W. E. *Inorg. Chem.* **1978**, *17*, 1758.
(20) McDonald, J. W.; Friesen, G. D.; Rosenhein, L. D.; Newton, W. E. *Inorg. Chim. Acta* **1983**, *72*, 205.
(21) Christou, G.; Mascharak, P. K.; Armstrong, W. H.; Papaefthymiou, G. C.; Frankel, R. B.; Holm, R. H. *J. Am. Chem. Soc.* **1982**, *104*, 2820. Christou, G.; Garner, C. D. *J. Chem. Soc., Dalton Trans.* **1980**, 2354.
(22) Averill, B. A.; Herskovitz, T.; Holm, R. H.; Ibers, J. A. *J. Am. Chem. Soc.* **1973**, *95*, 3523.
(23) Lane, R. W.; Ibers, J. A.; Frankel, R. B.; Papaefthymiou, G. C.; Holm, R. H. *J. Am. Chem. Soc.* **1977**, *99*, 84. Lane, R. W.; Ibers, J. A.; Frankel, R. B.; Holm, R. H. *Proc. Natl. Acad. Sci. U.S.A.* **1975**, *72*, 2868.
(24) McDonald, J. W.; Friesen, G. D.; Newton, W. E. *Inorg. Chim. Acta* **1980**, *46*, L79.
(25) Foss, O.; Jahr, J. *Acta Chem. Scand.* **1950**, *4*, 1560. Foss, O. *Inorg. Synth.* **1953**, *4*, 88.
(26) Lytle, F. W.; Greegor, R. B.; Sandstrom, D. R.; Marques, E. C.; Wong, J.; Spiro, C. L.; Huffman, G. P.; Huggins, P. E. *Nucl. Instrum. Methods Phys. Res.* **1984**, *226*, 542.
(27) Stern, E. A.; Heald, S. M. *Rev. Sci. Instrum.* **1979**, *50*, 1579.

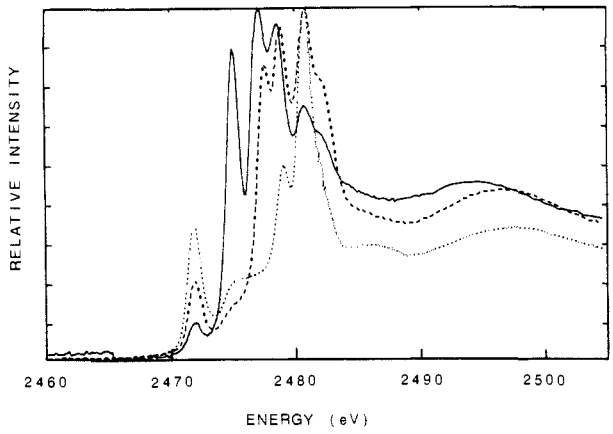

Figure 2. Sulfur K-edge XANES: freshly made, anaerobic aqueous solution of sodium dithionite (solid line); 33-h-old aerobic aqueous solution of sodium dithionite (dashed line); aqueous solution of sodium thiosulfate (dotted line). All solutions were prepared to be 100 mM and were not buffered. The decomposition of dithionite into thiosulfate as one of the products is clearly visible in the intensity and energy changes for several of the transitions.

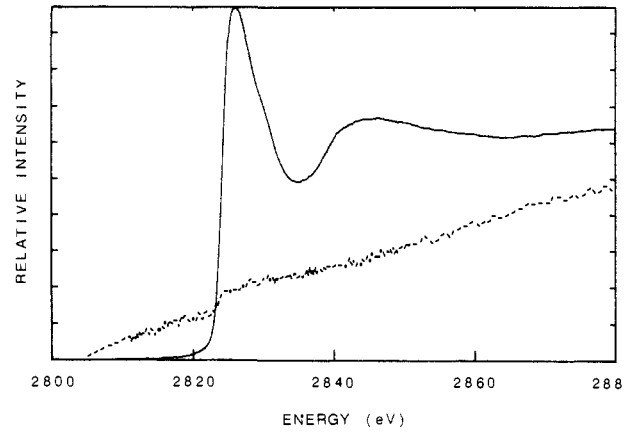

Figure 3. Chlorine K-edge XANES for dithionite-containing (solid line) and column-treated dithionite-free (dashed line) FeMo-co. The intensity scale of the dithionite-free spectrum has been expanded 10-fold to show the absence of any chlorine K white line in the column-treated sample. The minute edge jump matches that found for polypropylene, which was used as window material.

energy position of sulfur is very sensitive to formal oxidation state. We observe a 13-eV energy difference for formally S^{2-} (in MoS_4^{2-}) to S^{6+} (in SO_4^{2-}). An average shift of 1.6 ± 0.2 eV/unit increase in formal oxidation was observed for sulfur within a graded series of covalent compounds.[28] The magnitude of these shifts in sulfur K-edge spectra is coupled with a general structure-determined richness in edge features. These factors make XANES at the sulfur K edge an excellent tool in structure determination,[29] allowing identification of sulfur atoms having different oxidation states and electronic environments within the *same* compound.

The sulfur K-edge XANES spectra of the FeMo-co samples are shown in Figure 1. For samples A and B, the XANES of dithionite and its oxidation/decomposition products dominate and obscure the features originating from sulfur in FeMo-co. We have measured XANES of dithionite as a solid and as both an aged aerobic aqueous solution and a fresh anaerobic aqueous solution (Figure 2). The XANES of the fresh anaerobic solution changed over the course of each 15-min scan, with the intensity of most transitions changing at variable rates relative to each other, along with shifts in the apparent position of several lines, reflecting a complex decomposition. The spectra in Figure 2 clearly indicate $S_2O_3^{2-}$ as one of the decomposition products. We can, on the basis of these spectra, identify most peaks for FeMo-co samples A and B in Figure 1 as having the same position and line width as those of solutes originally derived from dithionite. The exception is the ~2470-eV feature, which has no equivalent in the dithionite spectra.

The XANES of the dithionite-free FeMo-co sample C show no overlapping features with the dithionite-related spectra, which indicates that the column filtration procedure indeed removed all dithionite, its decomposition products, and other small, unbound molecules and ions. This conclusion was confirmed by measuring and comparing chlorine K-edge XANES spectra for FeMo-co samples A and C (Figure 3).[30] The chlorine spectrum shows essentially complete removal of Cl^- by the column. This ion contaminant derives from HCl used during the cofactor isolation process. The minor edge jump present in the spectrum from sample C matches that found for pure polypropylene, which was used as window material.

The XANES of dithionite-free sample C is dominated by four transitions: two near 2470 eV and two around 2480 eV (Figure 1). The position of the major low-energy transition, at 2470.4 eV, corresponds to the unique feature in the spectra of samples A and B. The line widths of the FeMo-co transitions are the same as those for the ~2470- and ~2473-eV transitions deriving from Mo–Fe–S dicubane clusters, albeit at a slightly lower energy (0.4 and 0.8 eV, respectively; Figure 4a).

Inspection of the spectra in Figure 4b reveals that total sulfur is reflected in the intensity of the first continuum peak near 2477 eV. Comparison of spectra 1 and 2 shows that the presence of thiolate sulfur liganded to iron invariably results in a transition near 2473 eV. In the spectrum of $Fe_4S_4(SCH_2C_6H_5)_4^{2-}$ (Figure 4b (3)) this transition is clearly present but is diminished in intensity relative to the continuum peak since thiolate constitutes only half of the total sulfur in the molecule. Corroborating this assessment, the 2473-eV peak is absent from the spectrum of $Fe(MoS_4)_2^{3-}$, which has only sulfides.[31]

The transition at ~2470 eV can contain contributions from both types of liganding sulfurs (spectra 1, 3, and 4, Figure 4b). The thiolate-derived intensity is dependent on the oxidation state of the contained iron (spectra 1 and 2). Therefore, for iron–sulfur cluster compounds, the absolute intensity of this peak depends in a complicated way both on the average iron valence and on the ratio of sulfide to thiolate sulfur. In addition, comparison of spectra 2 and 4 shows that the ratio of the intensities of the characteristic peak to continuum peak is near unity for thiolate but approaches 1.3 for sulfide. Thus, it may be possible to estimate the relative numbers of the two types of sulfur donors in a cluster of unknown structure by deconvoluting the various features in the XANES spectrum. The observation of both these transitions in the FeMo-co spectrum indicates the presence of both sulfur types, sulfide and thiolate-like, in this molecule.

The two peaks at higher energy, 2478.2 and 2481.5 eV, can only result from sulfur in a high oxidation state with oxygen as part of its coordination sphere. The 2478.2-eV peak corresponds to an oxidation level of "3+" if the shift/oxidation relationship reported earlier is used.[28] If these FeMo-co transitions are assumed to originate from two separate types of sulfur atoms, the closest correspondence, among compounds investigated so far with a single white line, is found with SO_3^{2-} (2478.6 vs 2478.2 eV for FeMo-co) and cysteic acid (2481.3 vs 2481.5 eV for FeMo-co). The comparison with SO_3^{2-} is not reasonable, however, since this moiety would likely be bound to FeMo-co through its sulfur lone-pair electrons. This interaction would shift the transition energy maximum toward higher energy (as is seen for the sulfur of cysteic acid, for example, which is covalently attached to carbon[28]). We have found no other compound with a *single* white line in this

(28) Frank, P.; Hedman, B.; Carlson, R. M. K.; Tyson, T. A.; Roe, A. L.; Hodgson, K. O. *Biochemistry* **1987**, *26*, 4975.
(29) Spiro, C. L.; Wong, J.; Lytle, F. W.; Greegor, R. B.; Maylotte, D. H.; Lamson, S. H. *Science (Washington, D.C.)* **1984**, *226*, 48.
(30) The chlorine K edge is at ~2825 eV for Cl^-; chlorine K edges show high sensitivity to oxidation state changes (a maximum change of about 13 eV for the compounds we have investigated so far).
(31) Coucouvanis, D.; Simhou, E. D.; Baenziger, N. C. *J. Am. Chem. Soc.* **1980**, *102*, 6644.

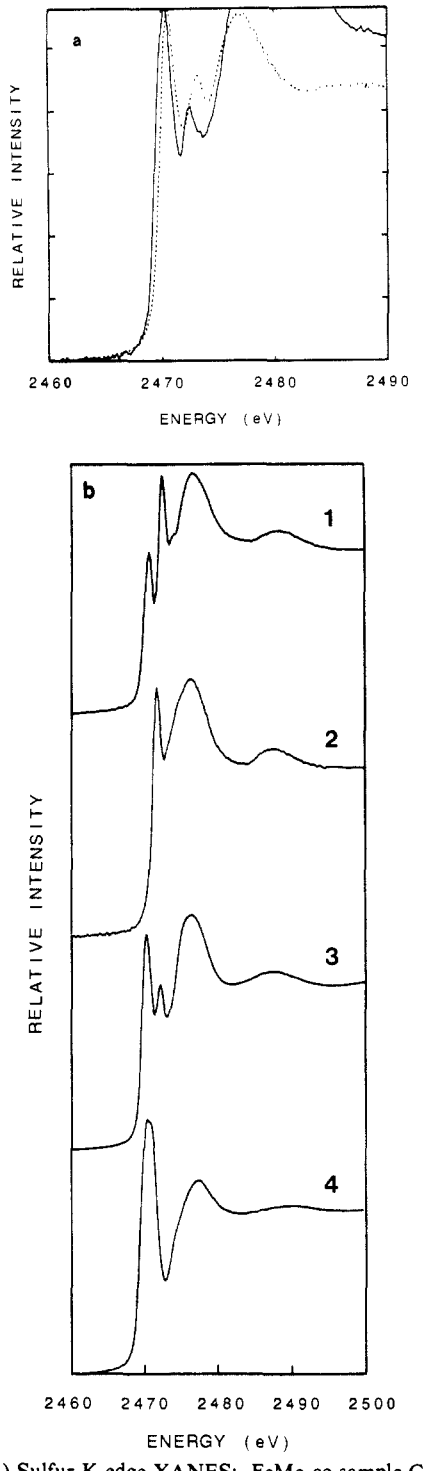

Figure 4. (a) Sulfur K-edge XANES: FeMo-co sample C (solid line) and $[Mo_2Fe_6S_8(OCH_3)_3(SC_6H_5)_6]^{3-}$ (dotted line), showing the similarity in line widths but the small differences (0.4 and 0.8 eV) in edge position for the first and second transitions respectively. The intensity scale of the FeMo-co spectrum has been adjusted to match the height of the first transition with that of the model. (b) Sulfur K-edge XANES: (1) $Et_4N[Fe(S_2\text{-}o\text{-}xyl)_2]$; (2) $(Et_4N)_2[Fe(S_2\text{-}o\text{-}xyl)_2]$ [Note the loss of the ~2470 eV feature on reduction of iron.]; (3) $(Et_4N)_2[Fe_4S_4(SCH_2C_6H_5)_4]$; (4) $(Et_4N)_3[Fe(MoS_4)_2]$. The edge jump is normalized to be 1 for all spectra.

energy region among the more than 80 sulfur-containing compounds investigated so far.

If *both* transitions are assumed to originate from the *same* species, a striking match is found between this FeMo-co spectrum and that of $(NH_4)_2Se(S_2O_3)_2\cdot 1.5H_2O$ (Figure 5). The $Se(S_2O_3)_2^{2-}$ anion has the symmetric structure $O_3S'\text{–}S''\text{–}Se\text{–}S''\text{–}S'O_3$, where the two unique S atom types give rise to three transitions. If analogy is made to our results[13] from Xα calculations of $S_2O_3^{2-}$,

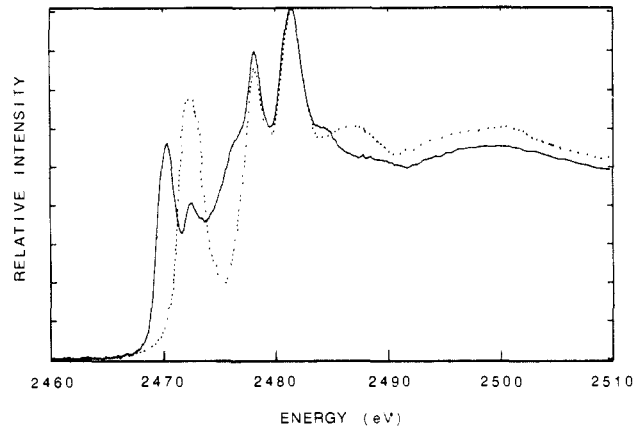

Figure 5. Sulfur K-edge XANES of dithionite-free FeMo-co sample C (solid line) and $(NH_4)_2Se(S_2O_3)_2\cdot 1.5H_2O$ (dotted line). The positions of the two high-energy transitions in the spectrum of $Se(S_2O_3)_2^{2-}$ overlap exactly those in the spectrum of FeMo-co. However, although the positions of the lower energy transitions near 2472 eV are comparable, their respective intensities are not[33] (see text).

the two high-energy transitions involve the S′ ground states. The first peak of $Se(S_2O_3)_2^{2+}$ near 2472.4 eV cannot, however, fully account for the analogous transition in the FeMo-co spectrum, even if the difference in self-absorption between FeMo-co (in dilute solution) and $Se(S_2O_3)_2^{2-}$ (solid) is taken into account.[32] However, the binding of an $-SSO_3$ moiety to Fe or Mo in FeMo-co would more likely be reminiscent of a ligating thiolate.[33] Its energy is close to that of elemental sulfur (2472.7 eV) and might indicate a covalently bound sulfur at a formal oxidation state close to 0. As discussed above, this same transition is also present in the XANES of all the Mo–Fe–S dicubane and Fe–S cubane clusters investigated (see, for example, Figure 4). In the FeMo-co spectrum, this transition, although not unambiguously assignable, may originate from the thiolate-like nature of the terminal sulfur of bound SSO_3^{2-}.

It is very worthwhile repeating that, in addition to the expected detection of transitions assignable to bridging sulfide, the two higher energy transitions definitively show the presence of sulfur atoms in higher oxidation states bound to oxygen as integral parts of FeMo-co sample C.

Molybdenum L Edges. The L_3 and L_2 edges, which represent transitions from $2p_{3/2}$ and $2p_{1/2}$ initial states, respectively, have a pronounced "white-line" feature assigned to the allowed $2p \rightarrow 4d$ transition.[34] For the large number of compounds we have studied (primarily ones containing molybdenum in oxidation state 5+/6+), the white line is generally split (we will assign α for the low- and β for the high-energy components) to a variable degree, reflecting a ligand field splitting of the d orbitals. For tetrahedral coordination the more intense component of the two white-line features is at higher energy, whereas for octahedral coordination it is at lower energy. Both the splitting and the relative intensities of the white-line features can be rationalized qualitatively by a simple ligand field approach. The relative intensities reflect the number of available orbitals, and the split reflects the energy difference for these orbitals in a tetrahedral vs an octahedral field.[34] It should be noted that the relative intensity order of the two

(32) In several cases, we have observed how self-absorption effects cause high-energy transitions to have a decreased intensity relative to low-energy transitions at high sample concentrations in solution, or in solids, relative to dilute solutions.

(33) The effect of coordination on decreasing the intensity and shifting the energy of the ~2472-eV transition may be gauged from the comparison of free thiosulfate (Figure 2) with its bound form in $Se(S_2O_3)_2^{2-}$ (Figure 5). Tetrathionate ($S_4O_6^{2-}$) shows a spectrum almost identical with that of $Se(S_2O_3)_2^{2-}$, but with a higher intensity and somewhat higher energy (2473.0 eV) for this discussed transition. Furthermore, the lower energy transition in the spectrum of $S_2O_5^{2-}$ is of significantly lesser intensity but occurs to higher energy (2475.6 eV) than the 2472.4-eV peak. In addition, a second peak (near 2477.8 eV) and a split third peak are observed for $S_2O_5^{2-}$ in the region of the high-energy peaks of $Se(S_2O_3)_2^{2-}$.

(34) Hedman, B.; Penner-Hahn, J. E.; Hodgson, K. O. *Springer Proc. Phys.* **1984**, *2*, 64.

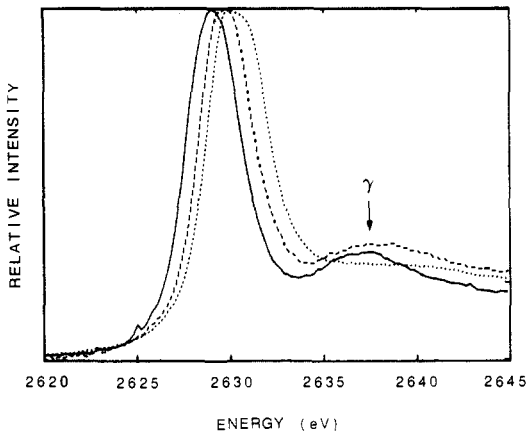

Figure 6. Molybdenum L_2-edge XANES for $Mo_2S_4(S_2CN(C_2H_5)_2)_2$ (solid line), $Mo_2O_2S_2(S_2CN(C_2H_5)_2)_2$ (dashed line), and $Mo_2O_4(S_2CN(C_2H_5)_2)_2$ (dotted line). The figure illustrates the change in edge position, and thus in the effective charge of the molybdenum atom with successive substitution of sulfur for oxygen in the coordination sphere. Note also the decrease in intensity of feature γ with an increasing number of oxygen atoms.

transitions is in general maintained when ligating oxygen is replaced by nitrogen and for mixed S/O ligation where short Mo–O bonds (~1.7 Å) are present.

There is a consistent difference in the relative intensity of the white-line features α and β between the L_3 and L_2 absorption edges. For every compound studied, the ratio of the α to β intensity is lower for L_3 relative to L_2.

A consistent increase in the energy of the L_3 and L_2 absorption edge positions is found as the formal oxidation state of molybdenum increases within a similar coordination geometry.[34] The increase is 0.4–0.6 eV/unit oxidation step, i.e. significantly less than that for the sulfur edge. The absorption edge energy position is also sensitive to a change in electronegativity of the ligand, as shown by the substitution of oxygen by sulfur in Figures 6 and 7. In general, both the α and β white-line features move to lower energy upon successive substitution with sulfur. At the same time, the energy separation between them decreases, reflecting the decreased ability of the softer ligand to split the energy levels. These shifts thus reflect a change in the effective charge of molybdenum, and they are of the same order of magnitude or larger than the shift caused by a unit formal oxidation state change for molybdenum with essentially unchanged ligation.

The first maximum, γ, in the near-edge region above the white line (Figures 6 and 7) is similarly sensitive to the type of nearest-neighbor atom to molybdenum. For several coordination geometries, this feature moves closer to the white line with increasing sulfur/oxygen ratio. Its maximum relative to the edge position follows approximately a $1/R^2$ dependence (where R is the average Mo–ligand bond length),[35] reflecting the increase in average Mo–ligand bond distance with increasing amounts of sulfur. For most octahedrally coordinated compounds, this near-edge feature is sharper with high amounts of sulfur and is lower in intensity in an all-oxygen environment. These effects are probably due to the higher back-scattering power of sulfur compared to oxygen, and possibly to a larger spread in Mo–ligand distances when oxygen is involved.

We have measured the XANES of a series of Mo–Fe–S dicubane cluster compounds suggested as possible models for FeMo-co.[36] The molybdenum L_3 spectra of some of these compounds are presented in Figure 7. A formal oxidation state for molybdenum in these compounds has not been definitively established, although 3+ has been inferred by the difference between core charges and the average iron oxidation states determined by Mössbauer spectroscopy.[21] For $Mo_2Fe_6S_8(SR)_9^{3-}$ (**1**), the coordination geometry around molybdenum is distorted octahedral with three long (2.57-Å) and three short (2.36-Å) Mo–S distances.[37] For $Mo_2Fe_6S_8(OCH_3)_3(SR)_6^{3-}$ (**3**), the bridging thiolate sulfurs are replaced by oxygens, giving distorted-octahedral dimensions close to Mo–S = 2.34 Å and Mo–O = 2.12 Å.[38] We have also studied $Mo_2Fe_6S_8(SR)_9^{5-}$ (**2**), the 2e-reduced analogue of $Mo_2Fe_6S_8(SR)_9^{3-}$. This molecule serves as a useful probe for the "location" of the single electron added to each subcluster. Mössbauer spectroscopy of this pair indicates that the molybdenum oxidation state is effectively unchanged in each subcluster on redox and that only the iron atoms undergo reduction.[21]

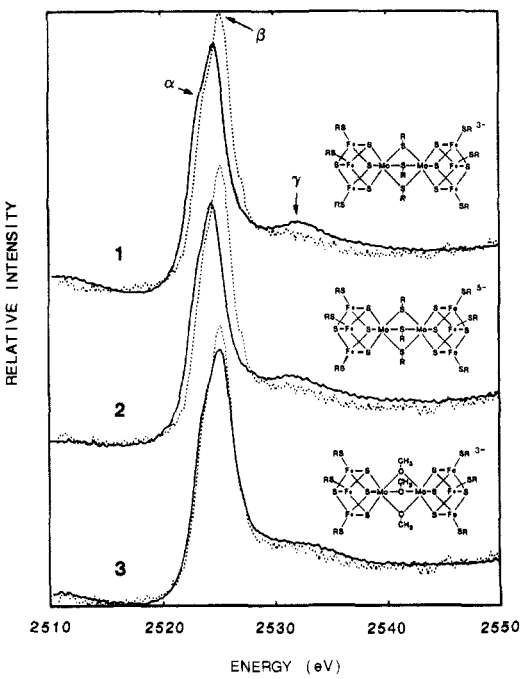

Figure 7. Molybdenum L_3-edge XANES for the cubane clusters $[Mo_2Fe_6S_8(SC_6H_5)_9]^{3-}$ (**1**), $[Mo_2Fe_6S_8(SC_6H_5)_9]^{5-}$ (**2**), and $[Mo_2Fe_6S_8(OCH_3)_3(SC_6H_5)_6]^{3-}$ (**3**). For comparison, the molybdenum L_3 XANES of the dithionite-free FeMo-co sample C is plotted with each spectrum as a dotted line. The best match in edge energy position and in intensity for feature γ is with the methoxy-bridged cluster 3.

The XANES of the dicubane models (Figure 7) are characterized by two closely spaced transitions (less than 1 eV), where the lower energy peak, α, is of lower intensity and appears as a shoulder on the higher energy white-line component, β. This situation is the opposite to that found for octahedral compounds of molybdenum in the 6+ and 5+ oxidation states. The white line of the dicubanes **1** and **2** is at a lower energy by about 2 and 5 eV, respectively, for the low-energy and high-energy inflection point compared to the corresponding features in the spectrum of $MoO_2(C_5H_7O_2)_2$. The variation in the differences for the two inflection points originates from the much larger split of the white line for $MoO_2(C_5H_7O_2)_2$.

There is no difference in either the edge position or line width for the clusters **1** and **2**, which differ only in redox state (Figure 7). The additional electrons appear not to reside on molybdenum, an observation consistent with other evidence (see above). For the methoxy-bridged cluster **3**, there is a ~0.7-eV shift relative to **1** if the maxima and high-energy inflection points are compared. The white line for **3** is however broadened by ~0.3 eV (3.6–3.9 eV), placing the low-energy side of the line at a position only ~0.4 eV higher than for **1**. It thus appears that the presence of oxygen, as before, shifts both transitions to higher energy and widens the splitting in their energy levels. However, the splitting here is lower in magnitude than that for the mononuclear molybdenum complexes.

(35) Natoli, C. R. *Springer Proc. Phys.* **1984**, *2*, 38.
(36) Holm, R. H. *Chem. Soc. Rev.* **1981**, *10*, 455.
(37) Christou, G.; Garner, C. D.; Mabbs, F. E.; King, T. J. *J. Chem. Soc., Chem. Commun.* **1978**, 740.
(38) Christou, G.; Garner, C. D.; King, T. J. *J. Chem. Soc., Chem. Commun.* **1979**, 503. This paper reports the tungsten analogue of this compound. The Mo–ligand distances are expected to be very close to the corresponding W–ligand distances.

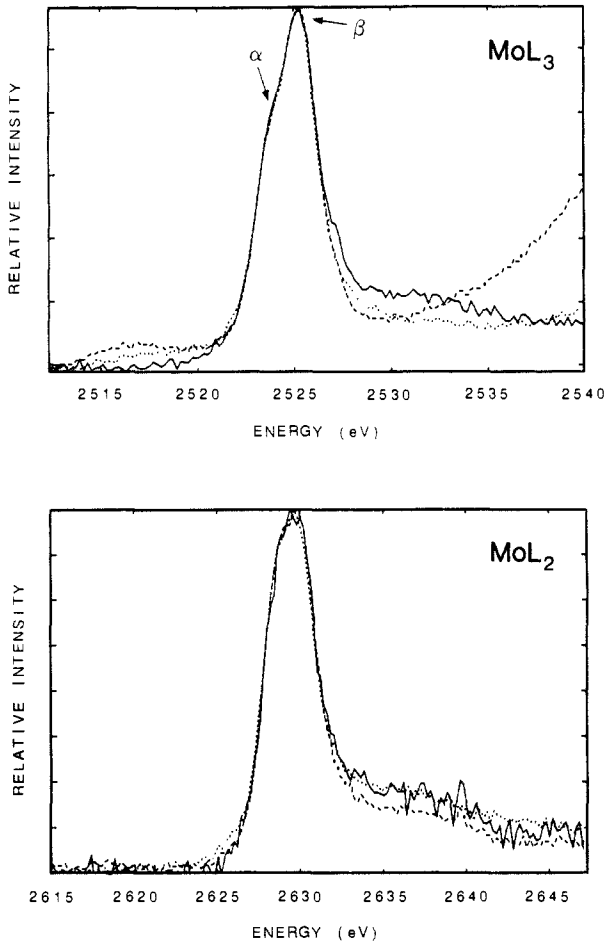

Figure 8. Molybdenum L_3- and L_2-edge XANES for FeMo-co samples A and B (both containing dithionite and/or it oxidation/decomposition products) and C (dithionite-free). In both parts of the figure, A is the dotted, B the dashed, and C the solid line. For the molybdenum L_3 spectrum, the sulfur K EXAFS and near-edge structure superimposes the molybdenum L_3 edge. These features give rise to abnormal pre- and postedge shapes that are impossible to subtract properly from the spectra of samples A and B. Note that the intensity ratio α/β is smaller at the L_3 edge as compared to at the L_2 edge.

The molybdenum L_3 and L_2 XANES spectra of the three FeMo-co samples A–C are superimposed in Figure 8. The white lines for all three samples are superimposable at both the L_3 and L_2 edges with respect to maximum and edge position, shoulder height, and line width. This result indicates that the column chromatography treatment has not modified the molybdenum center, which is consistent with the robust nature demonstrated by FeMo-co during anion-exchange chromatography.[6] More importantly, these observations show the molybdenum is not directly involved in the oxidized to semireduced redox change. In this respect the molybdenum in FeMo-co shows similarity to the behavior of that in the dicubane redox pair **1** and **2**. These results are in line with earlier EPR observations where no signal broadening was detected with a ^{95}Mo-substituted MoFe protein.[1] That observation suggested that molybdenum was not involved in the redox change of the FeMo-co cluster. However, recent ENDOR results[39,40] have demonstrated that molybdenum is an integral part of the cluster responsible for the EPR signal and that a broadening of only a few gauss in the EPR signal should be expected on ^{95}Mo substitution. This value would be too small to be observed by EPR. It could be that our failure to detect molybdenum L-edge shifts on redox may be due to the analogous

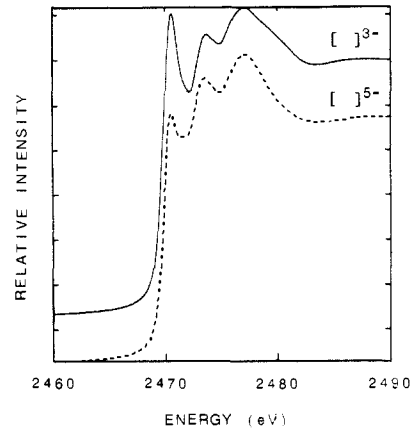

Figure 9. Sulfur K-edge XANES of $[Mo_2Fe_6S_8(SC_6H_5)_9]^{3-}$ (solid line) and $[Mo_2Fe_6S_8(SC_6H_5)_9]^{5-}$ (dashed line). The principal difference in the two compounds lies in the intensity of the first transition, which indicates that the extra two electrons are located in orbitals most likely involving both sulfur and iron, but *not* molybdenum (cf. text and Figure 7).

occurrence of a small shift below our detection limits. The situation would be exacerbated by a ligation change at molybdenum on redox, but there is presently no evidence to support this suggestion. Our interpretation of the XANES data is that at most there is only a small fractional electron density change at the molybdenum site.

As seen in Figure 7, the FeMo-co XANES of sample C is very similar in both shape, line width, and position to that of the cubane clusters. The fluorescence maximum energy is coincident with that of the methoxy-bridged cluster **3**. However, the line width is more similar to that of compounds **1** and **2**. The first feature γ in the near-edge region above the white-line for compounds **1–3** follows the trend described earlier. Thus, for **1** and **2** it is higher in intensity relative to γ in the spectrum of the methoxy-bridged cluster **3**. FeMo-co is very clearly most similar to **3** in this respect.

XANES Effects following Reduction. To obtain information concerning the specific redox-active site in a polynuclear cluster, there is a distinct advantage in studying two atomic types in the same compound under different redox states. The sulfur K XANES of the $[Mo_2Fe_6S_8(SC_6H_5)_9]^{3-}$ (**1**) and $[Mo_2Fe_6S_8(SC_6H_5)_9]^{5-}$ (**2**) clusters, which differ by one electron/subcluster, are compared in Figure 9. We noted above that there was no difference in the molybdenum L_3-edge spectra for these two anions. There is however a difference in the intensity of the first transition in the sulfur XANES. This observation indicates that the extra one electron/subcluster is located in an orbital having a sulfur-derived component and is clearly not localized on molybdenum. Other investigations have also suggested that sulfur is noninnocent during redox changes in polynuclear metal clusters.[41] We cannot make similar deductions from the present data with respect to changes in the FeMo-co sulfur XANES upon reduction because the sulfur K-edge spectrum of semireduced sample B was obscured by the presence of dithionite and related decomposition products. We are currently planning electrochemically controlled XANES measurements to probe the possibility of observing such an effect at the sulfur cluster sites in dithionite-free FeMo-co.

Conclusions

The experiments described above allow the following conclusions to be drawn with respect to FeMo-co.

1. All small, unbound molecules may be removed from NMF solutions of FeMo-co by means of anaerobic G-25 column chromatography, which in turn permits examination of the nature, oxidation state, and ligation characteristics of sulfur species directly bound to FeMo-co.

2. Three types of sulfur are associated with FeMo-co(ox) made dithionite-free by G-25 column chromatography: One is present

(39) Hoffman, B. M.; Roberts, J. E.; Orme-Johnson, W. H. *J. Am. Chem. Soc.* **1982**, *104*, 860.

(40) Venters, R. A.; Nelson, M. J.; McLean, P. A.; True, A. E.; Levy, M. A.; Hoffman, B. M.; Orme-Johnson, W. H. *J. Am. Chem. Soc.* **1986**, *108*, 3487.

(41) Müller, A.; Hellmann, W.; Newton, W. E. *Z. Naturforsch., B: Anorg. Chem., Org. Chem.* **1983**, *38b*, 528.

as sulfide and the other two represent thiolate-like and an oxidized sulfur species.

3. The sulfur K-edge features of the oxidized sulfur species on FeMo-co show close correspondence with those of bound thiosulfate. From the relative intensities of the various spectral features, it seems likely that at least one, or possibly more, S_2O_3-like moieties are bound. The presence of this anion as ligand may account for the overall negative charge of FeMo-co.[6] The presence of this ligand can also explain the thiolate-like feature in the XANES spectrum.

4. Chloride plays no part in ligation of iron or molybdenum in intact FeMo-co(ox).

5. The Mo atom is surrounded by a mixed sulfur and oxygen ligation sphere disposed in a distorted-octahedral manner. The close spectral correlation with the Mo–Fe–S dicubane clusters suggests a similar oxidation state for molybdenum, which may be best described as 4+ when recent ENDOR results are also considered.[39,40]

6. Comparison of the molybdenum L edges of both the oxidized and semireduced states of FeMo-co clearly shows the oxidation state of molybdenum is unchanged (at least within a small fraction of an electron) in this redox reaction.

7. Solutions of dithionite-free FeMo-co are stable in solution to X-ray-induced photoreduction. In contrast, solutions of FeMo-co(ox) containing dithionite-derived products (as well as chloride and possibly other unidentified molecules) completely photoreduce under the conditions of the XANES experiment within about 12 h.

As a result of these studies several major questions arise.

What is the source of the $S_2O_3^{2-}$? The simplest explanation is that it is produced during "self-oxidation" of FeMo-co, via the well-known disproportionation of $S_2O_4^{2-}$ into $S_2O_3^{2-}$ and HSO_3^-.[42] However, the possibility remains that the $S_2O_3^{2-}$ could derive from a novel ligand type intrinsic to the MoFe protein.

Is the unique ability of dithionite-containing NMF solutions to extract FeMo-co from the MoFe protein due to the presence of $S_2O_3^{2-}$ acting as a ligand? If so, then is dithionite itself necessary as a reductant? This situation could rationalize the recent extraction of FeMo-co into DMF or MeCN but only in the presence of $(Et_4N)_2S_2O_4$.[43] The Et_4N^+ salt of dithionite was noted as being particularly unstable in these solutions, suggesting the formation of considerable $S_2O_3^{2-}$.

Finally, if molybdenum is to play a major role in dinitrogen binding and reduction, why does it not receive the electron in the oxidized to semireduced reduction? Molybdenum must be included in subsequent electron transfers for the binding of the weakly π-acid dinitrogen molecule to be effective. Possibly then, the production of the sustained reducing (red) state involves electron transfer to molybdenum aided by energy-dependent conformational changes within the MoFe protein (driven by, e.g., interaction with the iron protein–ATP complex).

Acknowledgment. This work was supported by the National Science Foundation through Grant CHE 85-12129 to K.O.H. and by the National Institutes of Health through Grants RR1209 to K.O.H. and DK-37255 to W.E.N. Stanford Synchrotron Radiation Laboratory is supported by the Department of Energy, Office of Basic Energy Sciences, and the National Institutes of Health, Division of Research Resources.

(42) Danehy, J. P.; Zubritsky, C. W. III *Anal. Chem.* **1974**, *46*, 391. Cermák, V.; Smutek, M. *Collect. Czech. Chem. Commun.* **1975**, *40*, 3241. Kilroy, W. P. *J. Inorg. Nucl. Chem.* **1979**, *42*, 1071.

(43) Lough, S. M.; Jacobs, D. L.; Lyons, D. L.; Watt, G. D.; McDonald, J. W. *Biochem. Biophys. Res. Commun.* **1986**, *139*, 740.

NMR Study of the Conformations of Free and Lanthanide-Complexed Glutathione in Aqueous Solution

Benjamin Podányi and R. Stephen Reid*

Contribution from the Department of Chemistry, University of Saskatchewan, Saskatoon, Saskatchewan S7N 0W0, Canada. *Received July 30, 1987*

Abstract: The ^1H and ^{13}C NMR spectra of glutathione in its free and La(III)-complexed forms have been analyzed. The vicinal coupling constants were used to gain rotamer populations by the Karplus approach. The data were compared with the results of previous X-ray crystallographic, theoretical, and NMR studies. The gadolinium(III) complex of glutathione has been studied by the measurement of Gd(III)-induced ^1H and ^{13}C spin–lattice relaxation rate enhancements and application of the Solomon–Bloembergen equation. The two carboxylate groups of the molecule are found to be competing complexation sites; the microscopic formation constants have been determined. Complexation to the lanthanide(III) ions does not appear to change the conformational equilibrium of glutathione substantially.

Gadolinium(III) complexes are now widely used as "contrast agents" in nuclear magnetic resonance imaging.[1] An understanding of the specific relaxation rate enhancement of these paramagnetic complexes in different tissues, and of their toxicity, requires a detailed investigation of the behavior of Gd(III) complexes with biologically relevant molecules. We have therefore instituted a study of the stability and structure of such complexes in aqueous solution. The previous paper in this series[2] investigated the structure of amino acid and lactic acid complexes of Gd(III) using ^1H NMR relaxation rate enhancement measurements.

The present study concerns the Gd(III) complex of the tripeptide glutathione (γ-glutamylcysteinylglycine, GSH). GSH is a constituent of most cells, with several biochemical functions.[3] It is present at a concentration suitable for convenient NMR observation in vivo (for example, at approximately 2 mM in the human erythrocyte[4,5]). It possesses several potential metal-complexing sites. To our knowledge, no study of the Gd(III) complex has so far been reported in the literature.

We also consider here the solution conformations of free GSH. The conformation in the solid has been established by X-ray crystallography,[6] and possible conformations have also been

(1) Carr, D. H. *Physiol. Chem. Phys. Med. NMR* **1985**, *16*, 137.
(2) Reid, R. S.; Podányi, B. *Can. J. Chem.* **1987**, *65*, 1508–1512.

(3) Larsson, A.; Orrhenius, S.; Holmgrew, A.; Mannervik, B. *Functions of Glutathione*; Raven: New York, 1983.
(4) Ibbott, F. A. In *Clinical Chemistry*; Henry, R. J., Cannon, D. C.; Winkelman, J. W., Eds.; Harper and Row: New York, 1974; p 618.
(5) Brown, F. F.; Campbell, I. D.; Kuchel, P. W.; Rabenstein, D. L. *FEBS Lett.* **1977**, *82*, 12.

0002-7863/88/1510-3805$01.50/0